EXHIBIT 85

J Neuropathol Exp Neurol
Vol. 68, No. 2
February 2009
pp. 136–147

ORIGINAL ARTICLE

Hyaline Protoplasmic Astrocytopathy of Neocortex

E. Tessa Hedley-Whyte, MD, James E. Goldman, MD, PhD, Maiken Nedergaard, MD, PhD, Alan Friedman, PhD, Xiaoning Han, MD, Robert E. Schmidt, MD, PhD, and James M. Powers, MD

Abstract

Eosinophilic inclusions in the cytoplasm of protoplasmic astrocytes of the neocortex, usually in the clinical setting of epilepsy and/or psychomotor retardation, were first recognized and illustrated by Alois Alzheimer in 1910. Traditional special stains have failed to elucidate the specific nature of these inclusions. Ultrastructurally, the material was composed predominantly of highly electron-dense, non–membrane-bound, granular material distinct from Rosenthal fibers. Immunohistochemical examination has been informative but also sometimes inconsistent; it has recently been suggested that they may represent a filaminopathy (filamin A). We examined 5 cases with neocortical eosinophilic inclusions (3 autopsies, 2 surgical resections) using a standardized immunohistochemical protocol at a single institution. The specimens were immunostained with 32 antibodies to 30 potentially relevant proteins using several antigen retrieval protocols. We confirmed the presence of filamin A in these inclusions, but several additional proteins, particularly cytoglobin and glutamate transporter 1, were also identified. By electron microscopy in 2 cases, the granular fine structure of the inclusions was confirmed; mitochondria adjacent to, and perhaps within, the inclusions that contained many pleomorphic vesicular and membranous elements were also noted in 1 case. The pathophysiologic relevance of these proteins and the clinical significance of the hyaline inclusions are discussed.

Key Words: Cytoglobin, Glutamate, Hyalin, Inclusion, Proteomics, Protoplasmic astrocyte, Seizure

INTRODUCTION

Eosinophilic inclusions in the cytoplasm of protoplasmic astrocytes of the neocortex, usually in the clinical setting of epilepsy and/or psychomotor retardation, were purportedly first reported by Miyakawa et al in 1970 (1), Abe et al in Aicardi syndrome in 1992 (2), and Minagawa et al in polymicrogyric cortex in 1992 (3). We agree, however, with Špaček and Nožiča (4) that the keen morphologic eye of Alois Alzheimer was probably the first to recognize and illustrate these structures in the brain of a mentally impaired patient with epilepsy in 1910 (5). They also have been recognized in the excision specimen of a seizure focus from an otherwise neurologically intact patient (6). More recently, it has been suggested that they may represent a filaminopathy (7, 8). Van den Veyver et al (7) demonstrated the presence of filamin A in these astrocytic inclusions from 2 patients with Aicardi syndrome at autopsy. It is noteworthy that the filamin A was easily visualized only in the patient with a short postmortem interval. Hazrati et al (8) subsequently described the presence of filamin A in these inclusions in 5 surgical resections from patients with infant-onset seizures.

Traditional special stains have failed to elucidate the specific nature of these inclusions. To summarize, they are not argyrophilic by Bielschowsky, Bodian, and Gallyas techniques. They are almost always negative with periodic acid-Schiff (PAS) and Congo red and are negative with Cajal gold chloride technique, Alcian blue (pH not specified), calcium (Alizarin red and von Kossa), thioflavin T, orcein, and Azan-Mallory stains. They are slightly positive with acid fast (Ziehl Neelsen). They are ponceauphilic and positive with acid fuchsin, azocarmine, phosphotungstic acid–hematoxylin, and Holzer stains (1–4, 8). Ultrastructurally, all studies reveal the material to be composed predominantly of highly electron-dense, non–membrane-bound, granular material with each granule measuring approximately 30 nm in diameter (1–3, 6–9). Sometimes there is a membranous, vesicular, or filamentous component (1, 4, 8), and rough endoplasmic reticulum has been seen adjacent to or within the granular material (1, 9); however, RNAase does not dissolve them (6). All authors state that the inclusions are distinct from Rosenthal fibers, another refractile eosinophilic cytoplasmic inclusion seen mainly in fibrous astrocytes. Not surprisingly, immunohistochemical (IHC) examination has been most informative, but also sometimes inconsistent. The inclusions are reported to be negative with antibodies to glial fibrillary acidic protein (GFAP), ubiquitin, β-amyloid, neurofilament, polyglucosan, synuclein, microtubule-associated protein (MAP) 2, and α-B-crystallin (2–10). They are variably, usually weakly, immunolabeled for S-100, MAP 1b, and

From the Charles S. Kubik Laboratory for Neuropathology (ETH-W), Department of Pathology, Massachusetts General Hospital and Harvard Medical School, Boston, Massachusetts; Department of Pathology and Cell Biology (JEG), Columbia University, New York, New York; Center for Translational Neuromedicine (MN, XH), Division of Glial Disease and Therapeutics, Department of Neurosurgery, University of Rochester Medical Center, Rochester, New York; Department of Environmental Medicine (AF), University of Rochester Medical Center, Rochester, New York; Department of Pathology and Immunology (RES), Washington University School of Medicine, St. Louis, Missouri; and Departments of Pathology and Neurology (JMP), University of Rochester Medical Center, Rochester, New York.

Send correspondence and reprint requests to: James M. Powers, MD, Department of Pathology, University of Rochester Medical Center, Box 626, 601 Elmwood Ave, Rochester, NY 14642; E-mail: james_powers@urmc.rochester.edu

TABLE 1. Clinical Data

Case	1	2	3	4	5
Sex	F	M	M	F	M
Age at death/biopsy, years	14	7	26	14	4
Age of seizure onset	2–4 months	4 months	Unknown	Infant/7 years	4 months
Type of seizure	Gen/Myo	Gen/Myo	Unknown ≠	IS/Gen	Partial
Development	Severe delay	Severe delay	Unknown	Severe delay	Severe delay
Brain malformation	Single PVH	None	L Parietal Poly	None	None
Surgical resection	NA	NA	NA	R Frontal	R Frontotemporal
Postmortem interval	12 hours	20 hours	27 hours	NA	NA

≠, Available information indicates that he had a few intermittent seizures, the last at the age of approximately 20 years. However, there was severe head hitting behavior.
F, female; G, generalized; IS, infantile spasms; L, left; M, male; Myo, myoclonic; NA, not applicable; Poly, polymicrogyria; PVH, periventricular nodular heterotopia.

vimentin (6, 7, 9, 10); they are immunoreactive for filamin A (7, 8).

These enigmatic structures have been of interest to 2 of us (E.T.H.-W. and J.G.) for almost 3 decades and, more recently, to others for a variety of reasons (11). At Massachusetts General Hospital, the stainability of the inclusions from cases 1 and 2 was comparable to the reported results, except that phosphotungstic acid–hematoxylin was negative and PAS was positive (1 of 2). At Columbia University Medical Center (CUMC), immunostaining of cases 1 and 2 by J.G.

TABLE 2. Immunoperoxidase Antibody Data

Antibody	Source	Type	Dilution	Positive Control	Pretreatment
A. Manual Processing					
Albumin	Dako (Carpenteria, CA)	Antiserum	1:100	Umbilical cord	1
Biotin	Abcam (Cambridge, MA)	mAb	1:100	Kidney	1
Crystallin	Chemicon (Temecula, CA)	pAb	1:20000, 10000	Kidney	1, 2, 3
Cytoglobin	Santa Cruz (Santa Cruz, CA)	pAb	1:100	Pancreas	1, 2, 3
		mAb	1:600	Pancreas	1, 2
Hemoglobin	Dako	pAb	1:500	Blood clot	1, 3
Ferritin	Abcam	pAb	1:5000	Fetal liver	0
Filamin	RDI (Flanders, NJ)	mAb	1:500	Skin	1, 2, 3, 4
HO-1	Stressgen (Victoria, BC)	pAb	1:1000	AD Hpc	1, 2, 3
HO-2	Stressgen	pAb	1:5000	AD Hpc	1, 2, 3
HSP27	Chemicon	mAb	1:500	Kidney	0
HSP70	Abcam	mAb	1:500	Kidney	1
HSP90	Abcam	mAb	1:500	Kidney	1
Mitochondria (VDAC1/Porin)	Abcam	mAb	1:1000	Kidney	1, 2, 3
MnSOD	Stressgen	pAb	1:5000	Lung carcinoma	0, 1, 2, 3
Neuroglobin	Abcam	mAb	1:500	Pancreas	1, 2, 3
	Abnova (Walnut, CA)	pAb	1:100, 200	Pancreas	1, 2, 3
NAchR-α-4	Abcam	mAb	1:50	AD Hpc	1
Synuclein	Affiniti (Mamhead Exeter, UK)	pAb	1:20000	Lewy bodies	1, 2, 3
Ubiquitin	Chemicon	mAb	1:15000	AD Hpc	1, 2
B. Dako Autostainer					
GFAP	Dako	pAb	1:600	Astrocytoma	0, 2, 3
IgA	Dako	pAb	1:9000	Tonsil	2, 3
IgG	Dako	pAb	1:40000	Tonsil	2, 3
IgM	Dako	pAb	1:9000	Tonsil	2
Kappa	Dako	mAb	1:450	Tonsil	2
Lambda	Dako	mAb	1:350	Tonsil	2
S100	Dako	pAb	1:600	Sausage	citrate pH6, 2, 3
Vimentin	Dako	mAb	1:800	Sausage	2, 3

Pretreatments: 0, none; 1, Biocare Reveal; 2, proteinase K; 3, pepsin; 4, Biocare's Diva Decloaker per vendor's directions. Those antibodies listed with several pretreatments were initially subjected to the antigen retrieval system that worked best with the positive control, usually 0 or 1. When these failed or were equivocal, the enzymatic digestions were used with the proteins of high interest.

AD Hpc, Alzheimer disease hippocampus; GFAP, glial fibrillary acid protein; HO, heme-oxygenase; HSP, heat shock protein; Ig, immunoglobulin; mAb, monoclonal antibody; MnSOD, manganese superoxide dismutase; NAchR-α-4, nicotinic acetyl-cholinergic receptor alpha 4; pAb, polyclonal antibody; Sausage, a paraffin block containing cylindrical samples of multiple human organs; VDAC, voltage dependent anion channel.

revealed positive immunoreactivity for α-B-crystallin (±, few), heat shock protein (HSP) 27, ubiquitin (±) in only case 2, immunoreactivity for S-100 and GFAP in both, and no immunoreactivity for MAP 1b in either. A 1998 biopsy sample at CUMC (case 4) was immunoreactive for HSP27, α-B-crystallin, S-100 beta, and α-synuclein; negative for smooth muscle actin, tau (AT8), synaptophysin, and neurofilament; weakly immunoreactive for ubiquitin; and probably negative for GFAP. On the other hand, at Barnes Hospital of Washington University, the inclusions of case 5 showed no immunoreactivity for GFAP, neurofilament, neuroserpin, α-synuclein, or tau. They were negative with Bielschowsky impregnation and PAS, thioflavin S, and Luxol fast blue stains.

In view of the IHC inconsistencies between some of our earlier efforts and those reported in the literature, we decided to standardize the potentially relevant IHC studies by performing them in 1 institution, the University of Rochester/Strong Memorial Hospital (SMH). We also attempted to determine if there might be additional proteins in these inclusions that could play important pathophysiological roles. We provide ultrastructural data from 2 cases. We confirm the presence of filamin A in these inclusions, but several additional proteins, particularly cytoglobin and glutamate transporter 1 (GLT1), were identified. We also confirm the granular fine structure of the inclusions; in 1 case, mitochondria adjacent to, and perhaps within, the inclusions that contain many pleomorphic vesicular and membranous elements were also observed. The most persistent, and perhaps important, clinical questions that remain about these inclusions are as follows: Are they the cause of seizures? Are they the result of seizures? Are they the result of antiepileptic medications? Or do they occur pari passu with seizures? The data contained herein, we believe, contribute significantly to addressing these questions.

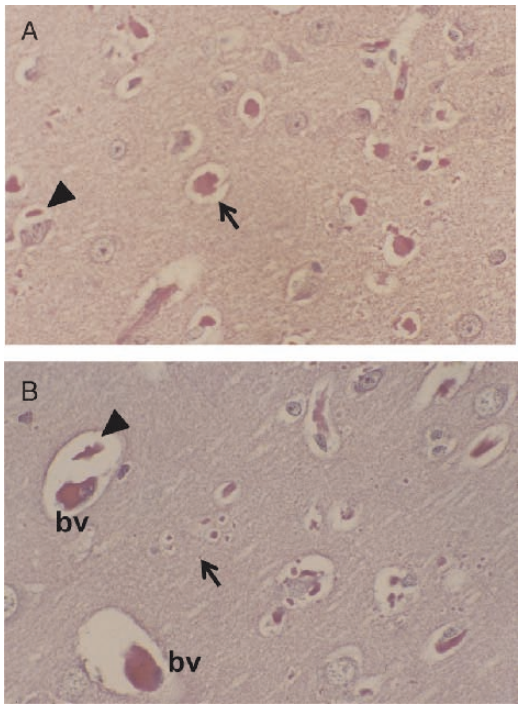

FIGURE 1. (A) Case 5. Hyaline inclusion within the cell body of a protoplasmic astrocyte (arrow) and in a satellite astrocyte (arrowhead). Hematoxylin and eosin (H&E); original magnification: 150×. **(B)** Case 5. Hyaline inclusions within the neuropil (arrow), as well as perivascular (arrowhead). Note the similar appearance of the inclusions to erythrocytes within blood vessels (bv) in both panels. H&E; original magnification: 150×.

Table 3. Immunohistochemical Labeling of Inclusions

Antibody	Case 1	Case 2	Case 3	Case 4	Case 5
A. Manual Processing					
Albumin	+	+	+	0	+
Biotin	0	0	0	0	0
Crystallin	+	+	+	+	+
Cytoglobin	+	+	+	+	+
GLT1	+	+	+	NA	+
Hemoglobin	0	0	NA	0	0
Ferritin	0	0	0	0	0
Filamin	+	+	+	+	+
HO-1	0	0	NA	0	0
HO-2	0	+	+	0	+
HSP27	NA	NA	NA	±	+
HSP70	NA	NA	NA	+	+
HSP90	NA	NA	NA	0	+
Mitochondria (VDAC1/Porin)	±	0	±	0	±
MnSOD	0	0	NA	0	0
Neuroglobin	±	0	NA	0	0
NAchR-α-4	0	0	0	0	0
Synuclein	0	0	NA	0	0
Ubiquitin	0	0	NA	0	0
B. Dako Autostainer					
GFAP	±	±	0	0	0
IgA	+	0	+	0	0
IgG	+	0	+	0	+
IgM	0	0	0	0	0
Kappa	0	0	+	0	0
Lambda	0	0	+	0	0
S100	±	±	+	0	0
Vimentin	0	±	0	0	0

0, negative; ±, equivocal or peripheral and probably in astrocytic cytoplasm; +, positive (see text for more details); GFAP, glial fibrillary acidic protein; GLT1, glutamate transporter 1; HO, heme-oxygenase; HSP, heat shock protein; Ig, immunoglobulin; MnSOD, manganese superoxide dismutase; NA, not applicable; NAchR-α-4, nicotinic acetylcholinergic receptor alpha; VDAC, voltage dependent anion channel.

MATERIALS AND METHODS

The cases used in this study, with some brief demographic and clinical information, are listed in Table 1. Cases 1 and 2 are 1988 and 1963 autopsy cases from Massachusetts General Hospital. Case 3 is an autopsy consultation that arrived at SMH while this study was in progress. Case 4 is a biopsy from CUMC in 1998. Case 5 is a biopsy that was received at SMH from Barnes Hospital of Washington University in 2006. Case 5, briefly fixed and containing a

plethora of hyaline inclusions, was the most informative specimen because it was amenable to several enzymatic digestion studies and a proteomic analysis. In addition to hematoxylin and eosin (H&E), stains for copper (rubeanic acid), calcium (Van Kossa), and iron (Perls Prussian blue) were performed in all cases with appropriate positive controls.

The main focus of our study was IHC. The antibodies, with or without specific antigen retrieval methods, are listed in Table 2. We initially searched for several groups of proteins that we considered as potentially relevant to the formation or breakdown of the inclusions: (1) astrocytic-GFAP, vimentin, S-100, biotin (covalently linked to the astrocytic glycolytic enzyme, pyruvate carboxylase), and GLT1; (2) stress proteins—heat shock 27, 70, and 90; α-B-crystallin; heme-oxygenase (HO) 1 and 2; manganese superoxide dismutase (MnSOD); cytoglobin; and neuroglobin; (3) synaptic-GLT1, nicotinic acetyl-cholinergic receptor alpha 4, and synuclein; (4) electron-dense granular material—albumin, hemoglobin, ferritin, immunoglobulin (Ig) A, IgG, IgM, kappa, and lambda; and (5) degradative-ubiquitin and filamin A. We later chose a mitochondrial antibody (VDAC/Porin) because of our ultrastructural findings. Our routine manual retrieval method is Biocare Reveal (Biocare Medical, Concord, CA) per the vendor's directions, with the exception that we perform a routine deparaffinization. This was our initial retrieval method for most manual procedures (#1 in Table 2). The proteinase K (PK) retrieval (#2 in Table 2) was Dako #S3020 (Dako, Carpinteria, CA) for 5 minutes at room temperature. The pepsin (Sigma P-7000) pretreatment consisted of 0.4% pepsin-HCl for 30 minutes at 40°C (#3 in Table 2). To ensure uniformity in the processing, all studies were performed at SMH on standard 6-μm-thick deparaffinized sections either manually by 1 technician in batches or on an automated Dako stainer in batches (cases 1, 2, 4, and 5). Case 3 was subjected to specific immunostains (those that were positive in the other

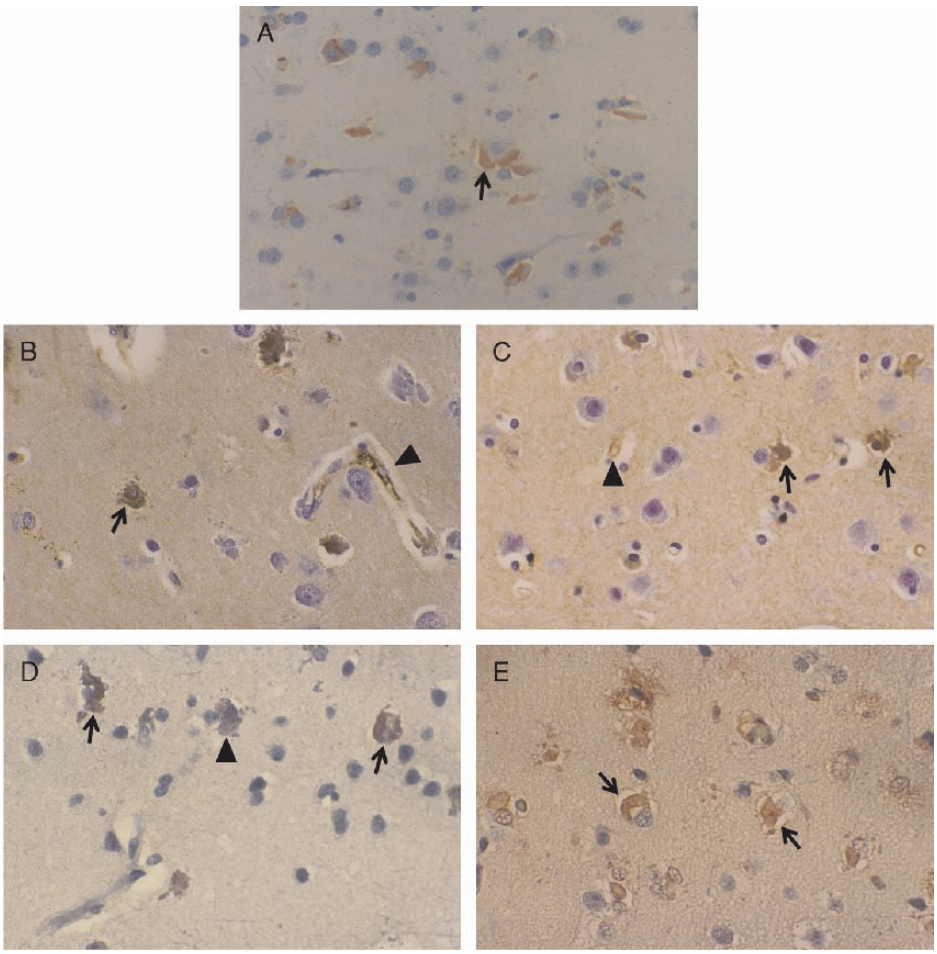

FIGURE 2. (A) Case 5. Immunoreactivity for filamin A (arrow). Anti-filamin A, retrieval, and 3-amino-9-ethyl carbazole (AEC); original magnification: 150×. **(B)** Case 1. Immunoreactivity for immunoglobulin (Ig) A (arrow) with internal control staining in a blood vessel (arrowhead). Anti-IgA, pepsin, and AEC; original magnification: 150×. **(C)** Case 3. Immunoreactivity for IgG (arrows) with weak internal control staining in blood vessel (arrowhead). Anti-IgG, proteinase K, and AEC; original magnification: 150×. **(D)** Case 3. Some inclusions are immunoreactive for hemoxygenase (HO) 2 (arrows), whereas another is not (arrowhead). This was a common occurrence with all antibodies. Anti-HO-2, retrieval, and AEC; original magnification: 150×. **(E)** Case 5. Immunoreactivity for heat shock protein (HSP) 70 (arrows). Anti-HSP70, retrieval, and AEC; original magnification: 150×.

cases), always with at least 1 of the positive cases to ensure reproducibility and consistency. The antigen detection system consisted of streptavidin-biotin complex with 3-amino-9-ethyl carbazole. In an attempt to reproduce the universal labeling of the inclusions with the antibody to filamin A (8), we also repeated the protocol as published (i.e. 1:100 dilution, avidin-biotin complex [ABC] with 3,3′-diaminobenzidine [DAB]). All immunostains had appropriate positive and negative (primary antibody omitted) controls.

The GLT1 assays were performed in a separate laboratory (M.N.). The slides from cases 1 to 3 and 5 were washed with 0.1 M phosphate-buffered saline (PBS) and blocked with 0.5% X-100 Triton containing 10% normal donkey serum. The initial sections of cases 1 and 5 had been pretreated with pepsin and PK, respectively. Later sections of case 1 received no retrieval. The sections of cases 2 and 3 were pretreated with retrieval and pepsin (case 2) or retrieval and PK (case 3). A mouse monoclonal antibody against GFAP (1:500, G3893; Sigma, St Louis, MO) and guinea pig anti-GLT1 (1:5000, AB5320; Chemicon, Temecula, CA) were applied overnight at 4°C. Immunoreactivities were revealed with affinity-purified CY3-conjugated anti–guinea pig and CY5-conjugated anti-mouse antibodies (1:250; Jackson Labs Bar Harbor, ME). After the immunolabeling, the sections were counterstained with 4,6-diamidino-2-phenylindole (1:10,000, D-21490; Invitrogen, Carlsbad, CA). Fluorescent signals were detected with a confocal microscope (FV500, Olympus) or a fluorescence microscope. To guarantee that the immunolabeled structures were the hyaline inclusions, the same slides from cases 1 and 5 used for confocal or fluorescence microscopy were subsequently stained with eosin or H&E and photographed for an exact comparison.

One evaluator (J.P.) assumed primary responsibility for the morphologic assessments. The data were then shared with all authors. Three of us (X.H., M.N., J.P.) independently and then jointly evaluated the GLT1 preparations. Electron micrographs were provided in cases 1 and 5 by E.T.H.-W. and R.S. using standard electron microscopic protocols. Finally, copper grids stained with uranyl acetate and lead citrate from cases 1 and 5 were subjected to electron probe microanalysis in a Hitachi 7650 transmission electron microscope with EDAX (EDAX, Inc, Mahwah, NJ).

Proteomic Analysis

Fifteen serial sections of case 5 were deparaffinized. Five slides were placed in PBS, 5 in the same PK solution for 5 minutes used in the IHC assays, and 5 in the same pepsin solution for 30 minutes at 40°C. One slide from the PK solution and 1 from the pepsin solution were taken and stained with H&E. All 3 solutions were then subjected to a modified proteomic analysis. The author responsible for this portion of the study (A.F.) was initially blinded to the IHC results. After the chromatographs were generated, correlations with the IHC data were attempted.

Samples were extracted 3 times with a 0.1% trifluoroacetic acid 50:50 water/acetonitrine mixture. These extractions were combined for each condition. The combined extracted solutions for each condition were subjected to solid phase extraction (SPE) to remove salts. After SPE, each condition was tested with matrix-assisted laser desorption/ionization and liquid chromatography–mass spectrometry (LC-MS) to determine the proteins extracted. The SPE desalting step was repeated 3 times before reasonable peptide signals could be observed. Linear ion trap (LTQ) spectra were acquired in positive ion mode, as previously described (12, 13). Proteins applied to LTQ were applied to a microcapillary liquid chromatography system (Surveyor MS Pump Plus HPLC system; Thermo Corporation, San Jose, CA) coupled to the LTQ. An in-line analytical capillary

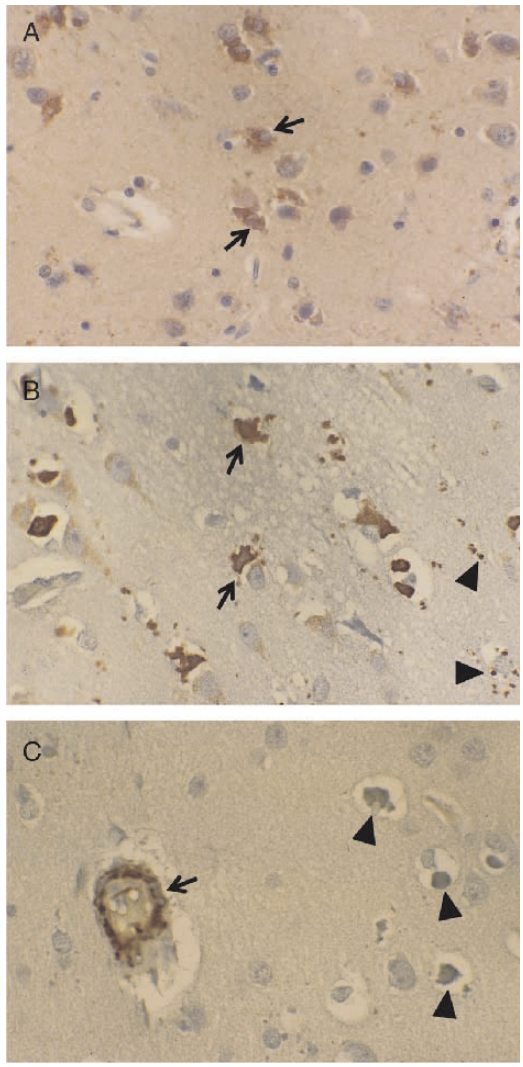

FIGURE 3. (A) Case 1. Immunoreactivity for cytoglobin (CGB) (arrows), mostly in astrocytic cell bodies. Anti-pCGB, pepsin, and 3-amino-9-ethyl carbazole (AEC); original magnification: 150×. **(B)** Case 5. Immunoreactivity for CGB in cell bodies of astrocytes (arrows) and in neuropil (arrowheads). Anti-pCGB, proteinase K (PK), and AEC; original magnification: 150×. **(C)** Case 5. In contrast to CGB, the filamin immunoreactivity of the inclusions (arrowheads) is lost after PK pretreatment, whereas the filamin immunoreactivity of the arteriole persists (arrow). The same was true for α-B crystallin. Anti-filamin A, PK, and AEC; original magnification 150×.

column (75 μm infecting dose, 10 cm) were home packed using C_{18} reversed-phase resin (5 μm, 200 Å Magic C_{18}AG; Michrom BioResource, Auburn, CA) and capillary tubing (75 μm infecting dose, 10 cm; Polymicro Technologies LLC, Phoenix, AZ) pulled to <10-mM open point using a P-2000/F (Sutter Instruments, Novato, CA). Samples were loaded on their own individual columns using a home-built pressure bomb. Peptides were eluted using a linear gradient of 5% to 70% solvent B (to a final working concentration of 0.1% formic acid in a solution of 95% acetonitrile and 5% water for 45 minutes), with a flow rate of 0.200 nL/minute across the column. The LTQ was operated in the data-dependent mode to automatically switch between MS, MS/MS, and neutral loss-dependent MS3 acquisition. Survey full-scan MS spectra (from/*z* 400 to 2,000) were acquired by LTQ. The 7 most intense ions were sequentially isolated and are fragmented in the linear ion trap using collision-induced dissociation. The data-dependent neutral loss algorithm in the Xcalibur software was enabled for each MS/MS spectra. Data-dependent settings were chosen to trigger an MS3 scan when a neutral loss of 98, 49, or 32.7 Da (to detect possible phosphorylation) was detected among the 10 most intense fragment ions. Former target ions selected for MS/MS were dynamically excluded for 30 seconds. The normalized collision energy using wideband activation mode was 35% for both MS2 and MS3. Ion selection thresholds were set at 500 counts for MS2 and 10 counts for MS3. The MS/MS spectra acquired on the LTQ were sequence database searched using SEQUEST and Bioworks Browser (both from Thermo Corporation) against the publicly available non-redundant Human sequence databases from the European Bioinformatics Institute (http://www.ebi.ac.uk/IPI/IPIhuman.html) to determine possible sequence correlations of known proteins with variable carbamidomethyl cysteine, oxidized methionine, and phosphorylation modifications. Default threshold cutoffs were made using the following parameters: normalized cross-correlation score for +1, +2, and +3 charge peptides of 1.9, 2.7, and 3.5 respectively, and a ΔCN value of 0.1.

RESULTS

Routine Light Microscopy

Histologic (H&E) stains generally confirmed previous reports. In brief, brightly eosinophilic, refractile (glassy) inclusions were noted within the cell bodies of protoplasmic astrocytes, both apparently isolated and as perineuronal satellite cells (Fig. 1A); these were more frequent than small neuropil deposits that were more frequent than perivascular deposits (Fig. 1B). They often had semilunar or horseshoe shapes, particularly when they were paranuclear or perineuronal; they occasionally surrounded astrocytic nuclei

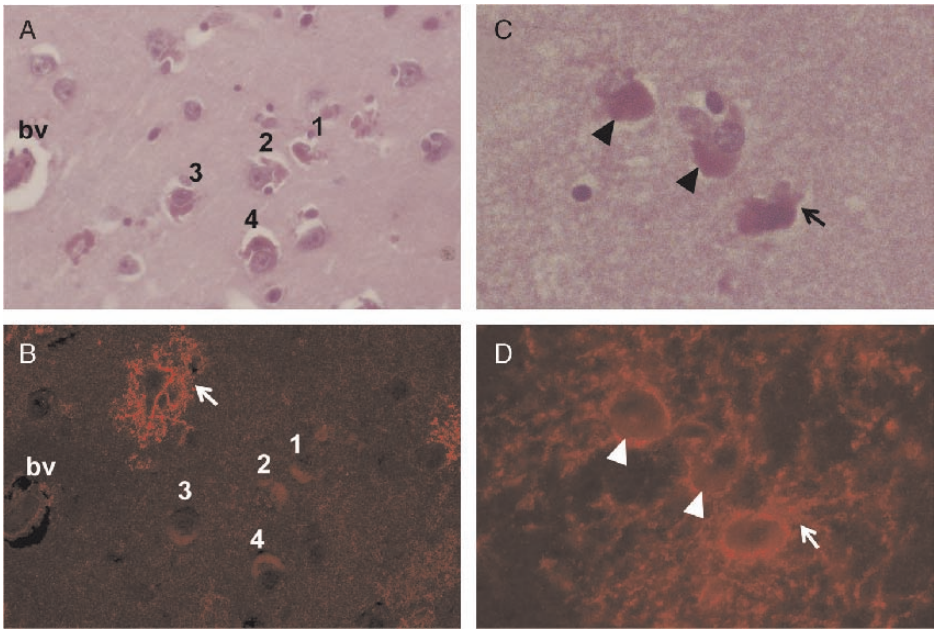

FIGURE 4. (A) Case 1. A cortical area with several astrocytes containing eosinophilic hyaline inclusions (1–4) near a blood vessel (bv). Hematoxylin and eosin (H&E); original magnification: 150×. **(B)** Confocal image of the same cortical area from the same slide and field as in **A** immunoreacted against glutamate transporter 1 (GLT1) (red). Note that only 1 astrocyte in the field expresses a high level of GLT1 (arrow). GLT1 in this astrocyte without a hyaline inclusion in the H&E-stained image is distributed evenly across the cell body and some of its proximal processes. The fine processes that are present in the neuropil of controls and case 5 are not labeled. The characteristic hyaline inclusions (1–4) label weakly with the GLT1 antibody. Anti-GLT1, no retrieval; original magnification: 150×. **(C)** Case 1. Three inclusions in the molecular layer (arrowheads and arrow). H&E; original magnification: 300×. **(D)** Confocal image of the same area from the same slide as in **C** immunoreacted against GLT1 (red). Most of the inclusion material (arrowheads) is weakly immunoreactive compared with the background at the base of the left arrowhead. Immunoreactivity in 1 focus seems to extend into short and coarse astrocytic processes (arrow). Strong immunoreactive rings, perhaps delimiting the edges of astrocytic cell borders, are also noted. Anti-GLT1, no retrieval; original magnification: 300×.

completely (4). The neuropil deposits were most frequent in cases 2 and 5. As reported earlier (4), the inclusions often resemble clusters of erythrocytes in microvessels with H&E stain. They were observed in all layers of the neocortex, perhaps most frequently in layers 2 and 3. They were present in layer 1, but not in the pia limitans. In the autopsy samples (cases 1–3), these inclusions were widely dispersed in all neocortical areas, even distant from a suspected primary seizure focus, that is, the posterior periventricular nodular heterotopia of case 1 and the left parietal polymicrogyric cortex of case 3. They were equally prevalent in the other neocortical sections as in the left parietal polymicrogyric cortex of case 3, which was used for the IHC. They were occasionally noted in the basal ganglia of cases 1 and 2 and rarely in the hippocampus of cases 3 and 5; they were absent from all cerebral white matter, brainstem, and cerebellum. They did not stain for calcium, copper, or iron.

Immunohistochemical Findings

A few general comments are necessary: A surprisingly large number of proteins were identified in the hyaline inclusions by IHC (Table 3), but no antibody, irrespective of the antigen retrieval method used, immunostained all of the hyaline inclusions in a single slide. It is not clear whether this reflects real differences in protein composition or if it is artifactual and due to differences in mode of death, postmortem interval, type or duration of fixation in formaldehyde solutions, or variations in alcohol processing (reviewed in Reference [14]). The hyaline inclusions were also difficult to distinguish from erythrocyte-filled microvessels in the IHC preparations. Therefore, at least 3 separate fields per slide were evaluated before a negative result was accepted. It is also well known that different antigen retrieval systems may be necessary to optimize IHC staining (reviewed in Reference [15]), as was the case in this study. For example, cases 1 and 2 generally stained best with pepsin pretreatment, whereas PK pretreatment was most effective with case 5. Case 4 had the fewest inclusions; these were difficult to immunolabel and were the most sensitive (i.e. they dissolved) in all antigen retrieval protocols. For these reasons, we decided to forego GLT1 immunostaining of this specimen. The best antigen retrieval system for case 3 varied from antibody to antibody.

Some proteins could not be demonstrated in the hyaline inclusions, even with a variety of antigen retrieval methods. These included biotin, ferritin, hemoglobin, HO-1, IgM, MnSOD, nicotinic acetylcholinergic receptor, synuclein, and ubiquitin. Anti-GFAP rarely and weakly stained the periphery of the inclusions in cases 1 and 2, as did antivimentin in case 2. Anti-S100 staining was similar in cases 1 and 2 but was more effective with pepsin pretreatment. An antimitochondrial antibody rarely stained their periphery in cases 1, 3, and 5.

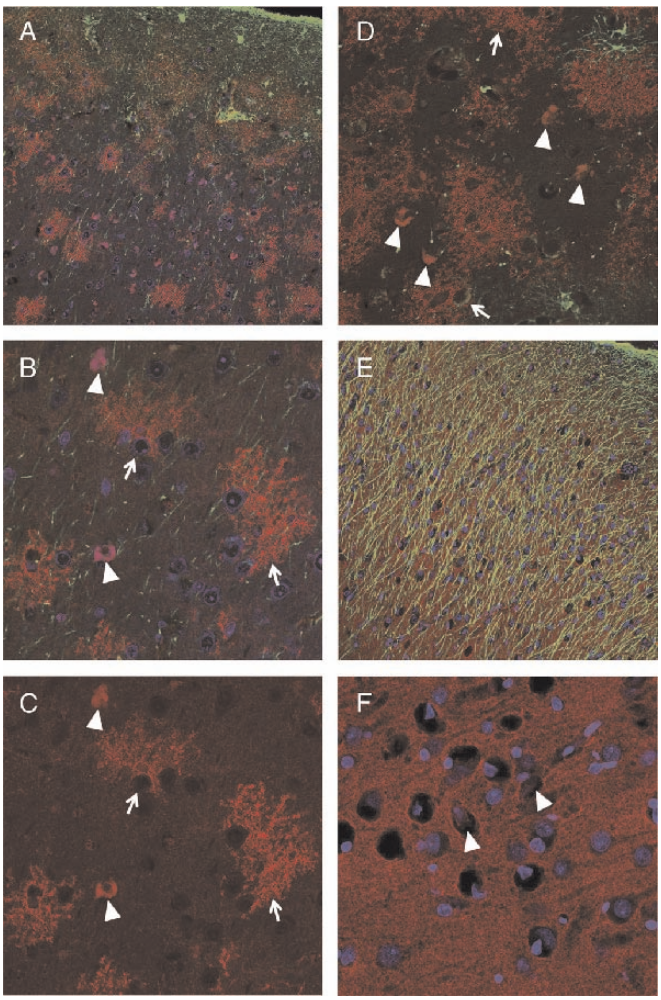

FIGURE 5. (A) Case 1. A low-power image shows that some cortical astrocytes exhibit a patchy expression of glutamate transporter 1 (GLT1) (red) in their cell bodies. In addition, there are numerous small pink-purple inclusions in areas with low GLT1 expression (right side and bottom of field). Anti-GLT1, anti-glial fibrillary acidic protein (GFAP), 4,6-diamidino-2-phenylindole (DAPI), pepsin; original magnification: 75×. **(B)** Higher power of panel **A** shows 2 inclusions (arrowheads); astrocytes with some proximal expression of GLT1 (red) are indicated by arrows. The few interlaminar astrocytic processes in cortical layers 2 and 3 are GFAP-positive (green). In contrast, no astrocytes in layer 2 or 3 are GFAP-positive; original magnification: 225×. **(C)** GLT1 labeling of same area as in panel **B**. Both the astrocytes (arrows) and inclusions (arrowheads) are labeled for GLT1. Anti-GLT1, pepsin; original magnification: 225×. **(D)** Case 3. Four inclusions (arrowheads) in astrocytes of layers 2 to 3 lacking immunoreactive arbors are labeled convincingly for GLT1 and interspersed among astrocytes with stunted arbors (arrows) and a paucity of GFAP-positive processes (green). Anti-GLT1, anti-GFAP; original magnification: 175×. **(E)** Case 5. A more normal area of superficial cortex shows the same subpial astrocytic staining (green at top) as in panel **A**. However, layers 2 and 3 contain a dense plexus of parallel interlaminar fibers that are positive for GFAP (green), which is typical of controls. Anti-GLT1, anti-GFAP, DAPI, proteinase K (PK); original magnification: 75×. **(F)** A higher magnification of the same area as in **E** demonstrates the normal fine background staining for GLT1 (red) and a few inclusions (arrowheads) that label weakly for GLT1. Anti-GLT1, DAPI, PK; original magnification: 225×.

We confirmed the presence of filamin in the hyalin inclusions in all cases (Fig. 2A), but this was usually weak and infrequent, even at 1:100 dilution with the ABC-DAB immunostaining procedure (8). The media of arterioles was always positive and more intensely stained than the inclusions. Microvessels (capillaries and venules) were variably immunoreactive and most prominent with ABC-DAB. Immunoglobulin A (Fig. 2B) was identified in the inclusions of cases 1 (with pepsin) and 3 (with PK or pepsin); IgG (Fig. 2C) was seen in cases 3 and 5 (with PK) and also in case 1 (with pepsin). Kappa and lambda immunoglobulin chains were only noted in case 3, particularly kappa (data not shown). Albumin was detected in cases 1 to 3 and 5, particularly cases 1 and 2 (data not shown).

Heme-oxygenase 2 (Fig. 2D) was diffusely present in cases 2 (with retrieval and particularly pepsin) and 3 (with retrieval) and focally seen in case 5 (particularly with PK). Of the heat shock proteins, performed only in cases 4 and 5, HSP70 was the most impressive, especially in case 5 (Fig. 2E). Heat shock protein 90 was also detected in case 5 with antigen retrieval, but not in case 4; HSP27 was equivocal in case 4 and rarely seen in case 5. Anti–α-B-crystallin rarely stained the inclusions of cases 4 and 5 at 1:20000, but more convincingly in cases 1 to 3 at 1:10000 with pepsin pretreatment (data not shown).

The easiest and most prominent protein identified in the inclusions was cytoglobin. It was seen in all cases, but particularly in cases 1 to 3 (with pepsin; Fig. 3A) and 5 (with PK; Fig. 3B). The monoclonal cytoglobin antibody was also applied to case 5: With retrieval, it was negative; with PK, it was focally positive. We also observed in case 5 that in contrast to the enhanced immunoreactivity of cytoglobin with PK, the immunoreactivity of filamin (Fig. 3C) and α-B-crystallin was lost with the same pretreatment. Antineuroglobin, monoclonal and polyclonal, was used multiple times and did not label the inclusions, except for weak staining of a few inclusions of case 1 (polyclonal with retrieval; data not shown).

Immunostaining for GLT1 was demonstrated in the inclusions of case 1 without retrieval (Figs. 4A–D). The inclusions stained more intensely with pepsin (cases 1 and 2) or PK (case 3) pretreatment (Figs. 5A–D). In cases 1 to 3, the inclusion-bearing astrocytes often had either stunted GLT1 arbors or lacked any demonstrable processes (Figs. 4B, D, 5A–D). The dense plexus of GFAP-positive interlaminar processes was severely reduced, and the normal fine-granular-background GLT-1 immunoreactivity of the neuropil was absent (Figs. 5A–D) when compared with the comparatively uninvolved cortex of case 5 (Figs. 5E, F) and normal murine controls (M. Nedergaard, personal observation). The inclusions in case 5 labeled weakly for GLT1 with PK pretreatment (Fig. 5F).

Electron Microscopy

The inclusions were almost entirely granular in case 1, but the inclusions of case 5 also contained much membranous and vesicular debris (Figs. 6A, B). The largest and most complex deposits in case 5 stood alone, presumably in astrocytic cell bodies with clear cytoplasm. Smaller and more purely granular deposits were found in the neuropil within small clear processes and rarely adjacent to small

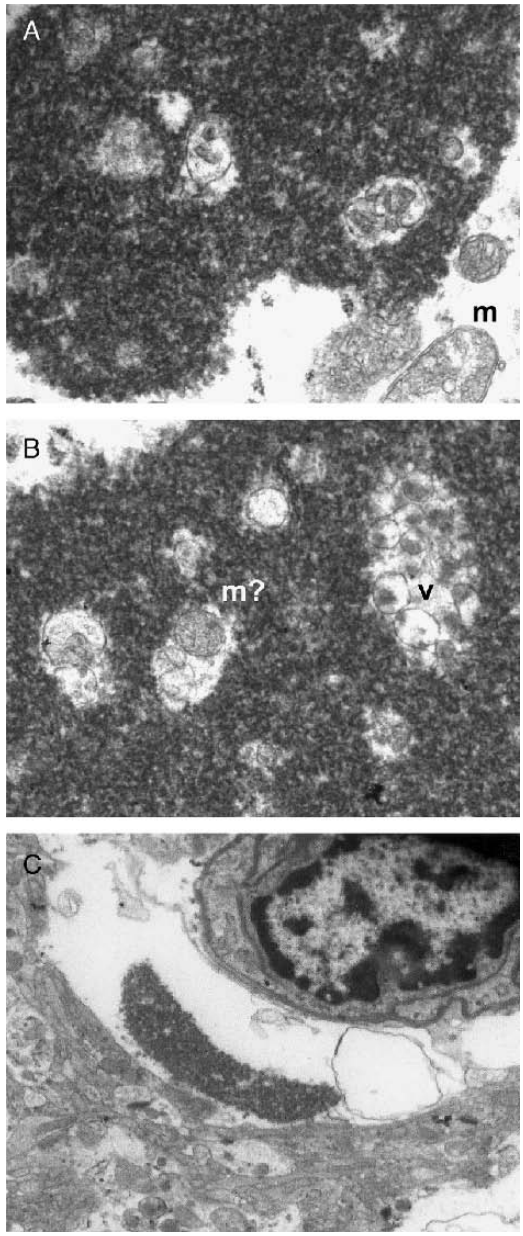

FIGURE 6. (A) Case 5. Electron-dense granules mixed with membranous elements; mitochondria (m) adjacent to inclusion. Uranyl acetate–lead citrate; original magnification: 30,000×. **(B)** Case 5. Another field showing a possible degenerating mitochondrion (m?) or autophagosome and a cluster of vesicles (v), measuring approximately 200 to 360 nm in diameter and containing dense cores. Uranyl acetate–lead citrate; original magnification: 30,000×. **(C)** This small inclusion is more purely granular and lies within an astrocytic process that directly abuts a small blood vessel (top right). The membrane discontinuity (top left) and the intracytoplasmic circular profile adjacent to the inclusion are of uncertain significance. Uranyl acetate-lead citrate; original magnification: 5,000×.

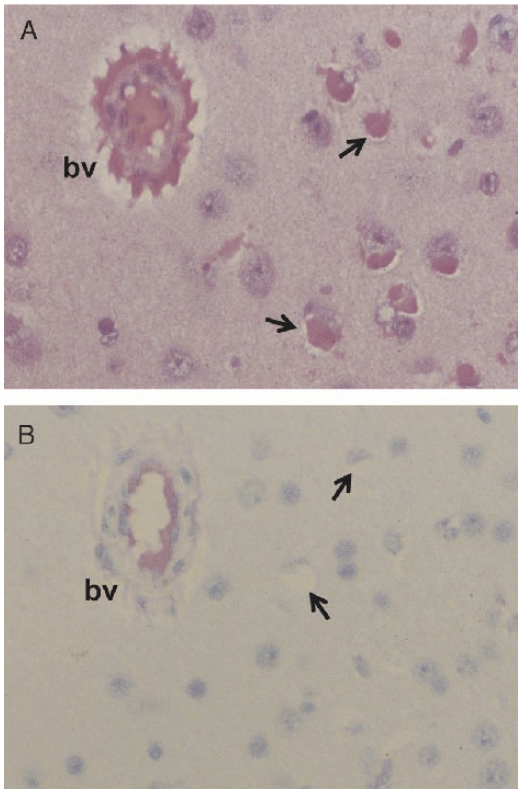

FIGURE 7. (A) Case 5. This slide was treated with proteinase K and then stained with hematoxylin and eosin (H&E). Note the preservation of the hyaline inclusions (arrows) and the similar appearance of erythrocytes within a blood vessel (bv). The normal eosinophilia of the neuropil has been muted. H&E; original magnification: 225×. **(B)** Same field as **A** with the same bv as a marker. This slide was treated with pepsin and then stained with H&E. Note that empty spaces (arrows) are all that remain of the hyaline inclusions. Also, the normal eosinophilic background of the neuropil is lost, suggesting that many proteins have been removed. H&E; original magnification: 225×.

blood vessels (Fig. 6C). Mitochondria were noted adjacent to and possibly within some of the deposits of case 5 (Fig. 6A).

Electron Probe Microanalysis

No abnormal peaks could be identified in case 1 or 5. Internal positive peaks included lead, from the lead citrate stain, and osmium, from the postfixation in osmium tetroxide.

Proteomic Analysis

The differential sensitivity of filamin, crystallin, and cytoglobin to PK treatment in the briefly formalin-fixed (i.e. less than 24 hours) case 5 allowed us to conduct a modified proteomic analysis. As shown in Figures 7A and B, the PK digestion did not alter the morphologic appearance of the inclusions, whereas pepsin dissolved them. We were unable to identify any of the proteins seen with IHC (Fig. 8), however. In the PBS extract, the 4 most abundant human proteins were collagen alpha-1 (III) chain precursor, methyl-CpG-binding domain protein 5, collagen alpha-1 (VII) chain

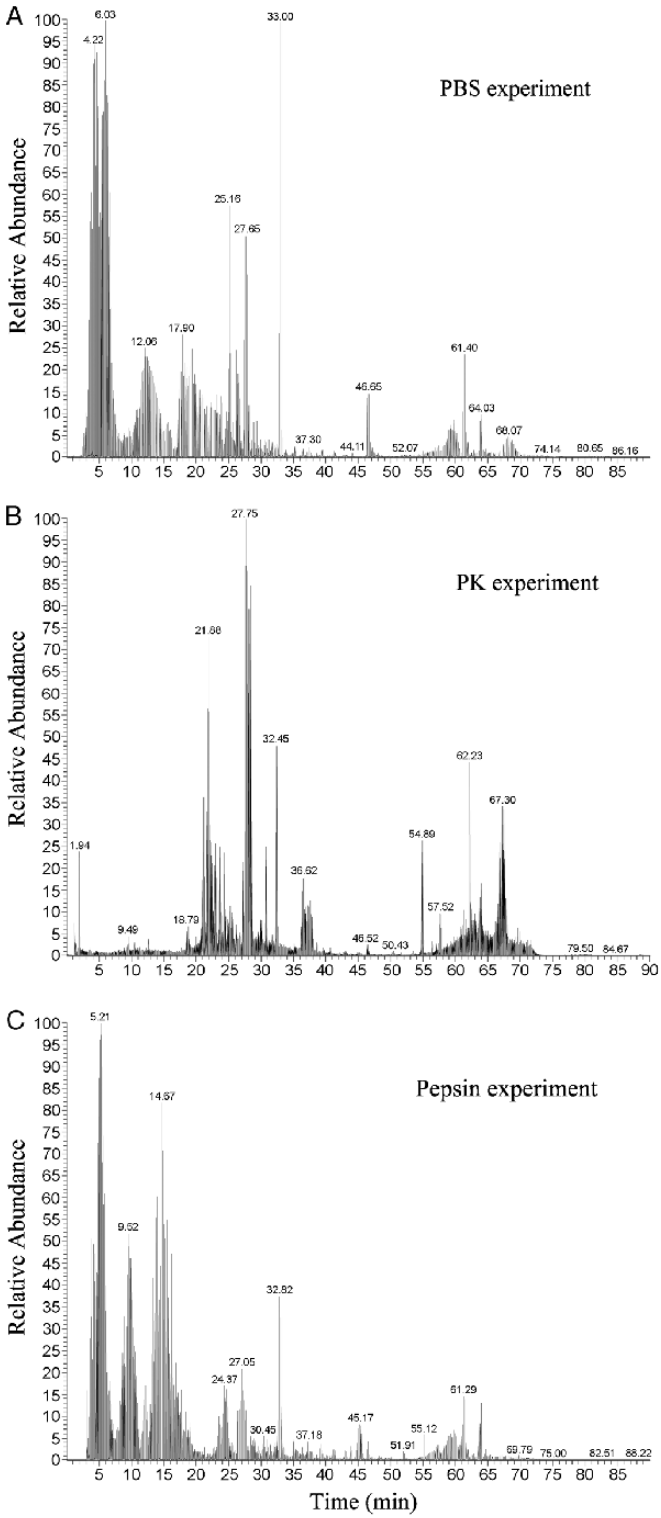

FIGURE 8. Case 5. Base peak chromatographs from the linear ion trap (LTQ) mass spectrometer of phosphate-buffered saline extraction **(A)**, proteinase K extraction **(B)**, and pepsin extraction **(C)** reveal that many characteristic peptides are present in the different extracts.

precursor, and activating signal cointegrator 1 complex subunit 3 (Fig. 8A). In the PK extract, we found thyroglobulin precursor, protein TAN C2, PWWP domain-containing protein 2A, and C-C chemokine receptor type 10 (Fig. 8B). In the pepsin extract, we noted collagen alpha-1 (I) chain precursor, RNA-binding protein MEX3D, laminin subunit β-4 precursor, and probable G-protein–coupled receptor 112 (Fig. 8C). In light of these findings, we then performed routine immunostains on the Dako autostainer to laminin (Dako, mAb Clone 4C7, 1:2K with PK, sausage internal control) and thyroglobulin (Dako, mAb Clone DAK-T5 6, 1:8K without retrieval, sausage internal control). None of our cases showed any labeling of the inclusions. The positive internal control immunostaining for laminin was vascular basement membranes.

DISCUSSION

This study confirms that filamin A is a component of the cytoplasmic inclusions in protoplasmic astrocytes of patients with seizures and/or psychomotor retardation, but we also have identified several other proteins. Cytoglobin may be the most prominent (i.e. much more than filamin A), but the presence of the astrocytic glutamate transporter (GLT1) may be the most important finding.

It is well established that the hyperactivity of neurons in a seizure focus results in energy depletion, with reductions in the substrates oxygen and glucose, the production of lactic acid, and the release of glutamate. Protoplasmic astrocytes of the neocortex play major roles in the normal homeostasis of cortical neurons, as well as in the control and perhaps generation of seizures (e.g. glutamate-glutamine cycling and Ca^{+2} release) (Reference [11], reviewed in References [16–18]). Those same astrocytes are the almost exclusive locus of the inclusions.

Of the additional proteins demonstrated by IHC, it seems likely that IgG, IgA, and albumin reflect an incidental uptake of serum proteins due to the proximity of astrocytes to brain microvessels, perhaps, that were more permeable because of the inclusions (Fig. 6C), seizures, or head trauma (e.g. head hitting behavior).

The presence of the inducible HSP70 in the inclusions is explicable on the basis of its known overexpression during epilepsy and other CNS insults, such as trauma (19). Small amounts of α-B-crystallin are also present. The presence of HO-2 in the inclusions may be related to its normal function as an oxygen sensor (20); HO-2 transcription levels are sensitive to hypoxia (reviewed in Reference [21]). It may be worthwhile, however, to recall that the main physiologic function of HO-2 is to cleave heme (Fe-protoporhyrin IX) from hemeproteins, such as cytoglobin. Hence, we might anticipate HO-2 in a pathologic brain inclusion containing cytoglobin. A parallel situation has been seen in hereditary ferritinopathy, in which hyaline inclusions have occurred extracellularly or in white matter glia, probably fibrous astrocytes. These inclusions contain HO-2, but also iron, ferritin, neuroglobin, and probably some cytoglobin (22, 23). In contrast to the present situation, however, there was abundant evidence of oxidative stress (e.g. the overexpression of HO-1 and MnSOD) and oxidative damage (22).

We confirmed that filamin A is present in the inclusions by IHC (7, 8) but could not reproduce the universal labeling of the inclusions that Hazrati et al (8) achieved, despite the fact that the standard streptavidin-biotin system we used is considered to be more sensitive than the ABC system (24). Dr Hawkins was kind enough to send us their galley proof while our study was underway, and we tried additional antigen retrieval methods, including one that is considered among the most powerful, that is, Biocare's Diva Decloaker. We could not appreciably increase our ability to label the inclusions with the same antibody and lot, even following the same protocol of Hazrati et al (8). We cannot explain these differences at this time.

We had greater success in labeling the inclusions with a polyclonal antibody to cytoglobin. These data along with the enhanced labeling with PK in case 5 versus the abolition of filamin immunoreactivity with the same pretreatment suggest that cytoglobin is a more abundant or intrinsic protein in the inclusions than filamin (or crystallin). This conclusion must be tempered, however, by the fact that the cytoglobin antibody used may have a greater affinity for its epitopes, which are located between amino acids 45 to 95 (Santa Cruz Biotechnology, Santa Cruz, CA; personal communication). These amino acids are within the cytoglobin core, which contains the secondary structure topological sites (25). Cytoglobin is the most recently discovered hemeprotein that is present in almost all human tissues, including the brain (26), where it seems to be upregulated in oxidative stress (27) and perhaps hypoxia (28–30). Another reason to suspect that cytoglobin is a—perhaps the—major protein in the inclusions is their morphologic resemblance to hemoglobin-containing erythrocytes (4; Figs. 1, 7A).

Unfortunately, our proteomic analysis did not confirm the presence of any protein demonstrated in the inclusions with IHC. Presumably, this is because their concentrations fall below the detectable level of our MS technique. To obtain such a correlation for a small intracytoplasmic proteinaceous aggregate probably would necessitate laser capture microdissection (31). The analysis did, however, confirm the feasibility of performing proteomics on briefly formalin-fixed, paraffin-embedded samples (32). Brief formalin fixation probably obviates many of the adverse effects of formaldehyde on proteins, including cross-linkages (14). We thought it unlikely that laminin or thyroglobulin precursor would be the main constituent of the inclusions, and neither protein was identified in the inclusions.

The possibly most important, but not necessarily abundant, protein identified in the inclusions was the astrocytic glutamate transporter, GLT1. This protein is most important because it may provide a partial answer to the questions posed earlier in "Introduction" concerning the clinical significance of the inclusions. First, we can disregard the consideration that the inclusions are a result of antiepileptic medication. The case of Alzheimer preceded the availability of such drugs, except perhaps phenobarbital, and the patient reported by Špaček and Nožiča never received such medications (4). In addition, one of us (J.G.) has seen these inclusions infrequently in other clinical situations (e.g. Alzheimer disease) in which clinical seizures were not

manifest nor were antiepileptic medications administered. Might they be coincidental or pari passu with seizures? This seems unlikely because most of the reported cases have had a strong seizure history.

Are the inclusions the cause or result of seizures? This is unanswerable at present, but we can offer some pathogenetic speculations. The autopsy data in those with localized seizure foci (e.g. cases 1 and 3) and their presence at autopsy in some patients without a seizure history (e.g. Alzheimer disease) (4) mitigate against the possibility that the inclusions cause seizures. If they are the result of seizures, which seems most probable, the seizures must be generalized or the inclusions are related to spreading depression, because the inclusions in the neocortex at autopsy are far removed from the suspected seizure foci. Case 3 has too little clinical data to contribute to this discussion, but cases 1 and 2 would support this contention. Nevertheless, countless patients with generalized convulsions do not exhibit these inclusions at biopsy or autopsy. There must, therefore, be some additional pathogenetic factor.

This does not exclude the possibility that the inclusions may be a morphologic marker of an underlying genetic defect that might be the cause of seizures, or that the inclusions may contribute to their progression. The intensity of the GLT1 immunoreactivity in the inclusions in cases 1 to 3 was enhanced by pepsin or PK pretreatment (compare Figs. 4B and 5C, D), similar to that of cytoglobin in case 5. This suggests that GLT1 also may be an internal protein of the inclusion. Many of the astrocytes that display the inclusions in cases 1 to 3 have a stunted or absent GLT1-immunoreactive arbor, as do others lacking the inclusions (Fig. 5A). Moreover, the diffuse immunoreactivity of the neuropil for GLT1 seen in case 5 and murine controls is reduced to absent in cases 1 and 3. This may be due to either a downregulation of GLT1 or a loss of the fine astrocytic processes. Perhaps, the membranous and vesicular debris seen in the inclusions of case 5 and other reports (1, 4) represent the remnants of astrocytic processes, an early sign of the degeneration of the protoplasmic astrocyte. Some of the vesicular structures with double-unit membranes (e.g. in Fig. 6B) also might represent autophagosomes (33), a common clearance mechanism for aggregated proteins, rather than degenerate mitochondria. Cases 1 to 3 were much older than case 5, suggesting that the loss or downregulation of GLT1 may progress over time. The inclusions are, however, just as prominent in patients with severe seizures (cases 1 and 2) as in those with milder forms of epilepsy (cases 3 and 5). In situations where chronic severe seizures are not evident or none are manifest, one might speculate that it is not the seizures or any seizure-associated structural lesion such as periventricular heterotopia per se that are inducing the inclusions, but any kind of excessive glutamatergic stress on the protoplasmic astrocytes. To support this hypothesis, one would need an additional constitutional, perhaps genetic, predisposition that would allow only certain epilepsy patients and a few nonepilepsy patients to be vulnerable to such an excitatory insult and develop the inclusions.

Might a genetic defect in cytoglobin or GLT1 in the astrocyte be the underlying cause of seizures in a subset of epilepsy patients who display these inclusions? In mice, at least, a deletion of the *GLT1* gene results in epilepsy (34). Irrespective of whether some genetic defect in GLT1 occurs in a subset of epilepsy patients, the loss of the astrocyte GLT1 processes or a stress-induced downregulation of GLT1 over time, combined with trapping of GLT1 in the inclusions, might result in even greater excesses of extracellular glutamate and the progression of the seizure disorder. Preliminary confocal studies in cases 1 and 3 using antibodies to both GLT1 and S100b demonstrate an even background staining for S100b around inclusion-bearing astrocytes that lack GLT1-immunoreactive arbors (data not shown). These data suggest that a total loss of astrocytic processes has not occurred and that a downregulation of GLT1 is the more likely pathogenetic event. It is important to emphasize, however, that the presence of inclusions seems to be independent of the downregulation of GLT1 or a loss of astrocytic processes, because case 5 with its intact GLT1 pattern (Figs. 5E, F) has as many inclusions per unit area available for study as cases 1 and 3.

Finally, on a semantic note, the term "eosinophilic" inclusions seems to be too imprecise and somewhat inappropriate because so many normal structures in the CNS are eosinophilic, including myelin, neuropil, collagen, smooth muscle, and so forth. Therefore, we propose the term "hyaline" for these inclusions to connote their pathologic nature and to be consistent with established pathologic terminology. The noun "hyalin" ("hyaline" is the adjective) has been defined as "an alteration within cells or in the extracellular space, which gives a homogeneous, glassy, pink appearance in routine sections stained with hematoxylin and eosin" (35). The last point is the tentative proposal of the nosologic term "filaminopathy," by Hazrati et al (8), for patients with these inclusions. In view of the multiplicity of proteins identified by IHC in our study, this designation seems premature. The more all-encompassing term "proteinopathy" is justified. We do not know, however, whether there is a consistent major protein in these inclusions and, therefore, believe that it would be imprudent to endorse a single protein (e.g. cytoglobin) at the present time.

ACKNOWLEDGMENTS

The authors thank Frances Vito for her talent and patience in performing the manual immunohistochemical stains, Jenny Smith for her graphic support, and both Tina Blazey and Linda Crandall for outstanding secretarial assistance. They also thank Karen Bentley, Ian Spinelli, and Ted Cocsis of AMETEK/EDAX for the electron x-ray spectroscopy.

REFERENCES

1. Miyakawa T, Sumiyoshi S, Deshimaru M, et al. Electron microscopic study on a case of idiocy: Astrocytes and mental deficiency. Acta Neuropathol 1970;16:25–34
2. Abe H, Yagishita S, Itoh K, et al. Novel eosinophilic inclusion in astrocytes. Acta Neuropathol 1992;83:659–63
3. Minagawa M, Shioda K, Shimizu Y, et al. Inclusion bodies in cerebral cortical astrocytes: A new change of astrocytes. Acta Neuropathol 1992; 84:113–16
4. Špaček J, Nožiča Z. Cytoplasmic inclusions in neocortical astrocytes

associated with arteriopathic encephalopathy and dementia. Hum Pathol 1994;25:1366–70
5. Alzheimer A. Beiträge zur Kenntnis der pathologischen Neuroglia und ihrer Beziehungen zu den Abbauvorgängen im Nervengewebe. In: Nissl F, Alzheimer A, eds. *Histlogische und Histopathologische Arbeiten über die Grosshirnrinde mit besonderer Berücksichtigung der pathologischen Anatomie der Geisteskrankheiten*. Jena: Gustav Fischer Verlag, 1910: 454–55
6. Horoupian DS, Hattab EM, Heit G. Astrocytic cytoplasmic inclusions within an epileptic focus in an otherwise neurologically intact patient. Hum Pathol 2003;34:714–16
7. Van den Veyver IB, Panichkul PP, Antalffy BA, et al. Presence of filamin in the astrocytic inclusions of Aicardi syndrome. Pediatr Neurol 2004;30:7–15
8. Hazrati L-N, Kleinschmidt-DeMasters BK, Handler MH, et al. Astrocytic inclusions in epilepsy: Expanding the spectrum of filaminopathies. J Neuropathol Exp Neurol 2008;67:669–76
9. Minamitani M, Tanaka J, Maekawa K. Peculiar eosinophilic inclusions within astrocytes in a patient with malformed brain. Brain Dev 1994;16: 309–14
10. Kato S, Hirano A, Umahara T, et al. Immunohistochemical studies on the new type of astrocytic inclusions identified in a patient with brain malformation. Acta Neuropathol 1992;84:449–52
11. Tian G-F, Azmi H, Takano T, et al. An astrocytic basis of epilepsy. Nat Med 2005;11:973–81
12. Parker KC, Patterson D, Williamson B, et al. Depth of proteome issues: A yeast isotope-coded affinity tag reagent study. Mol Cell Proteomics 2004;3:625–59
13. Elias JE, Haas W, Faherty BK, et al. Comparative evaluation of mass spectrometry platforms used in large-scale proteomics investigations. Nat Methods 2005;2:667–75
14. Fowler CB, O'Leary TJ, Mason JT. Modeling formalin fixation and histological processing with ribonuclease A: Effects of ethanol dehydration on reversal of formaldehyde cross-links. Lab Invest 2008;88: 785–91
15. Ramos-Vara J, Beissenherz ME. Optimization of immunohistochemical methods using two different antigen retrieval methods on formalin-fixed, paraffin-embedded tissues: Experience with 63 markers. J Vet Diagn Invest 2000;12:307–11
16. Hertz L, Peng L, Dienel GA. Energy metabolism in astrocytes: High rate of oxidative metabolism and spatiotemporal dependence on glycolysis/glycogenolysis. J Cereb Blood Flow Metab 2007;27:219–49
17. Wetherington J, Serrano G, Dingledine R. Astrocytes in the epileptic brain. Neuron 2008;58:168–78
18. Lovatt D, Sonnewald U, Waagepetersen HS, et al. The transcriptome and metabolic gene signature of protoplasmic astrocytes in the adult murine cortex. J Neurosci 2007;27:12255–66
19. Yang T, Hsu C, Liao W, et al. Heat shock protein 70 expression in epilepsy suggests stress rather than protection. Acta Neuropathol 2008;115:219–30
20. Williams SEJ, Wootton P, Mason HS, et al. Hemoxygenase-2 is an oxygen sensor for a calcium-sensitive potassium channel. Science 2004; 306:2093–97
21. Maines MD, Gibbs PEM. 30 some years of heme oxygenase: From a "molecular wrecking ball" to a "mesmerizing" trigger of cellular events. Biochem Biophys Res Commun 2005;338:568–77
22. Mancuso M, Davidzon G, Kurlan RM, et al. Hereditary ferritinopathy: A novel mutation, its cellular pathology, and pathogenetic insights. J Neuropathol Exp Neurol 2005;64:280–94
23. Powers JM. p53-mediated apoptosis, neuroglobin overexpression, and globin deposits in a patient with hereditary ferritinopathy. J Neuropathol Exp Neurol 2006;65;716–21
24. Shi Z-R, Itzkowitz SH, Kim YS. A comparison of three immunoperoxidase techniques for antigen detection in colorectal carcinoma tissues. J Histochem Cytochem 1988;36:317–22
25. de Sanctis D, Dewilde S, Pesce A, et al. Crystal structure of cytoglobin: The fourth globin type discovered in man displays heme hexacoordination. J Mol Biol 2004;336:917–27
26. Mammen PPA, Shelton JM, Ye Q, et al. Cytoglobin is a stress-responsive hemoprotein expressed in the developing and adult brain. J Histochem Cytochem 2006;54:1349–61
27. Li D, Chen XQ, Li W-J, et al. Cytoglobin up-regulated by hydrogen peroxide plays a protective role in oxidative stress. Neurochem Res 2007;32:1375–80
28. Schmidt M, Gerlach F, Avivi A, et al. Cytoglobin is a respiratory protein in connective tissue and neurons, which is up-regulated by hypoxia. J Biol Chem 2004;279:8063–69
29. Fordel E, Geuens S, Dewilde S, et al. Cytoglobin expression is upregulated in all tissues upon hypoxia: an in vitro and in vivo study by quantitative real-time PCR. Biochem Biophys Res Commun 2004; 319:342–48
30. Li RC, Lee SK, Pouranfar F, et al. Hypoxia differentially regulates the expression of neuroglobin and cytoglobin in rat brain. Brain Res 2006; 1096:173–79
31. Zhang J, Keene D, Pan C, et al. Review Article. Proteomics of human neurodegenerative diseases. J Neuropathol Exp Neurol 2008; 67:923–32
32. Crockett DK, Lin Z, Vaughn CP, et al. Identification of proteins from formalin-fixed paraffin-embedded cells by LC-MS/MS. Lab Invest 2005; 85:1405–15
33. Tang G, Yue Z, Talloczy Z, et al. Autophagy induced by Alexander disease-mutant GFAP accumulation is regulated by p38/MAPK and mTOR signaling pathways. Hum Mol Genet 2008;17:1540–55
34. Tanaka K, Watase K, Manabe T, et al. Epilepsy and exacerbation of brain injury in mice lacking the glutamate transporter GLT-1. Science 1997;276:1699–702
35. Cellular adaptations, cell injury and cell death. In: Kumar V, Abbas AK, Fausto N, eds. *Robbins and Cotran Pathologic Basis of Disease*. Philadelphia, PA: Elsevier Saunders, 2005:39

